

Applied Mathematics and Computation, Vol. 205, No. 2, 2008, pp 927-934

Palmprint Identification Using Restricted Fusion

Wei Jia^{1,2}, Bin Ling^{3*}, Kwok-Wing Chau⁴, Laurent Heutte⁵

¹Intelligent Computation Lab, Hefei Institute of Intelligent Machines, Chinese Academy of Science, PO Box 1130, Hefei, Anhui 230031, China

²Department of Automation, University of Science and Technology of China, Hefei, 230027, China

³Department of obstetrics and gynecology, Anhui Provincial Hospital, Anhui Medical University, Hefei 230001, China

Bin.ling88@gmail.com

⁴Department of Civil & Structural Engineering, Hong Kong Polytechnic University, Hong Kong, China

⁵Lab. LITIS, UFR Sciences, University of Rouen, France

Abstract. In this paper, we propose two palmprint identification schemes using fusion strategy. In the first fusion scheme, firstly, the principal lines of test image is extracted, and matched with that of all training images. Secondly, those training images with large matching scores are selected to construct a small training sub-database. At last, the decision level fusion, combing matching scores of principal lines and Locality Preserving Projections features, has been made for final identification in small training sub-database. From another point of view, it can be seen that the fusion is restricted by the previous results of principal lines matching, so we call it as restricted fusion. The second fusion scheme is similar to the first one. Just the fusion order is changed. The results of experiments conducted on PolyU palmprint database show that the proposed schemes can achieve 100% accurate recognition rate.

Keywords: Palmprint identification, Biometrics, Fusion, Principal lines, Locality Preserving Projections

1 Introduction

In information and networked society, automatic personal identification is an impending and crucial problem that needs to be solved properly. As an efficient and

* Corresponding author

safe solution, biometrics technology has recently been receiving wide attention from researchers. Similar to fingerprint or iris based personal identification, palmprint based identification system can also achieve good performance. For example, it can obtain high accurate recognition rates, and fast processing speed etc [1]. At the same time, palmprint based identification system has several special advantages such as stable line features, rich texture features, low-resolution imaging, low-cost capturing devices, easy self positioning, and user-friendly interface etc. For these reasons, nowadays the research related to this issue is becoming more active.

So far, there have been many approaches proposed for palmprint recognition including verification and identification, which can be divided into five categories.

(1) Texture based approaches have been studied extensively, which have shown good performance in terms of recognition rates and processing speed. Zhang and Kong proposed PalmCode method, which employed one 2D Gabor filter to extract the texture feature of palmprint [1]. Later, Kong et al. proposed FusionCode using feature-level fusion strategy, which can be regarded as the improved version of the PalmCode [2]. Chen et al. used dual-tree complex wavelets to extract texture energies of palmprint, and adopted SVM for classification [3]. Li et al. proposed a texture-based palmprint retrieval scheme using a layered search strategy for personal identification [4].

(2) Line based approaches are also important for palmprint recognition since lines are essential and basic features of palmprint. Zhang et al. used over-complete wavelet expansion and directional context modeling technique to extract principal lines-like features [5]. Han, et al. proposed using Sobel's and morphological operations to extract the line-like features from palmprint images [6]. Lin, et al. applied the hierarchical decomposition mechanism to extract principal palmprint features, which includes directional and multi-resolution decompositions [7]. Wu et al. regarded the palm lines as a kind of roof edges, and extracted them according to the zero-cross points of image's first-order derivative and the magnitude of the edge points' second derivative [8 9]. Liu et al. extracted the palm lines as a kind of wide lines [10 11]. Huang et al. proposed a modified finite radon transformation to extract principal lines [12].

(3) The research on appearance methods is an active area in pattern recognition field. And this technique was also applied to palmprint recognition. Lu et al. and Wu et al. proposed two methods based on Principal Components Analysis (PCA) and Linear Discriminant Analysis (LDA), respectively [13, 14]. Connie et al. proposed

several PCA/LDA/ICA-based approaches. And in order to analyze the palmprint images in a multi-resolution-multi-frequency representation, they also adopted wavelet transformation at the same time [15]. Moreover, Hu et al. employed 2D Locality Preserving Projections (2DLPP) for palmprint recognition [16]. Additionally, the Unsupervised Discriminant Projection (UDP) proposed by Yang, which was one of the variations of discriminant LPP, achieved satisfying recognition results [17].

(4) Orientation based approaches are deemed to have the best performance in palmprint recognition field, because orientation feature contains more discriminative information than other features, and is insensitive to illumination changes. A. Kong and D. Zhang were the first authors who investigated the orientation information of the palm lines for palmprint verification, which was defined as Competitive Code [18]. X.Q. Wu et al. proposed another orientation feature based approach named as POC using several directional filters to define the orientation of each pixel [19]. In addition, Ordinal Code proposed by Z.N. Sun et al. and Robust Line Orientation Code proposed by W. Jia were also using orientation feature for palmprint recognition [20 21].

(5) Recently, more and more multi-feature and multi-model based approaches using information fusion technologies have been proposed, since these approaches could provide more reliable results using more features. A. Kumar proposed a multi-feature based approach, which exploited three features, i.e. Gabor based texture feature, line feature and PCA feature [22]. Ribaric and Fratric proposed a biometric identification system based on eigenpalm and eigenfinger features, which extracted the PCA feature from both palm and finger ROI images [23]. A. Kumar proposed an approach combining hand shape and palmprint texture features [24]. T. Savic et al presented a multi-model system based on feature extracted from a set of 14 geometrical parameters of the hand, the palmprint, four digitprints and four fingerprints, which obtained very small equal error rate (EER) [25]. In [26], the knuckle-print was integrated a multi-model based scheme. J.G. Wang et al. investigated a novel approach exploited palmprint and palm vein using feature level fusion [27]. Jing et al proposed a fusion method combining face and palmprint in pixel level and used kernel DCV-RBF classifier for small sample biometrics recognition [28]. Zhao and Huang et al. proposed a recognition method using modular neural networks [29-33].

In this paper, we also propose a multi-feature based approach combining principal lines and LPP features for palmprint identification. As we know, the principal lines are the most important and stable feature, which can reflect the whole structure of

palmpoint. However, only using principal lines for palmpoint matching will lose other useful information. On the other hand, LPP feature can be regarded as the statistic feature of palmpoint. Thus, in our approach these two features can be jointly used to make a more reliable recognition scheme by exploiting their each advantage.

In this paper, all palmpoint images come from Hong Kong Polytechnic University Palmpoint Database, which were captured by a CCD-based device described in [1]. This paper is organized as follows. Section 2 presents the feature extraction methods. Section 3 describes the matching methods and fusion strategies. Section 4 reports the experimental results. Section 5 offers our concluding remarks.

2. Feature Extraction Based on the Modified Finite Radon Transform

2.1 Extracting principal lines using modified finite radon transform

In a palmpoint image, a palm line can be regarded as a straight line approximately in a small local area. Here, we design a modified finite radon transform (MFRAT) to extract line feature of palmpoint, which is defined as follows [12]:

Denoting $Z_p = \{0, 1, \dots, p-1\}$, where p is a positive integer, the MFRAT of real function $f[x, y]$ on the finite grid Z_p^2 is defined as:

$$r[L_k] = MFRAT_f(k) = \frac{1}{C} \sum_{(i,j) \in L_k} f[i, j] \quad (1)$$

where C is a scalar to control the scale of $r[L_k]$, and L_k denotes the set of points that make up a line on the lattice Z_p^2 , which means :

$$L_k = \{(i, j) : j = k(i - i_0) + j_0, i \in Z_p\} \quad (2)$$

where (i_0, j_0) denotes the center point of the lattice Z_p^2 , and k means the corresponding slope of L_k . In our paper, L_k has another expression $L(\theta_k)$, where

θ_k is the angle corresponding to k .

Note that before taking the transform given in Eq. (1), the mean should be subtracted from an input F , thus we have:

$$f = F - \text{mean}(F) \quad (3)$$

In the MFRAT, the direction θ_k and the energy e of center point $f(i_0, j_0)$ of the lattice Z_p^2 are calculated by following formula :

$$\theta_{k(i_0, j_0)} = \arg(\min_k (r[L_k])) \quad k = 1, 2, \dots, N \quad (4)$$

$$e_{(i_0, j_0)} = |\min(r[L_k])| \quad k = 1, 2, \dots, N \quad (5)$$

where $|\cdot|$ means the absolute operation.

In this way, two new images, Direction_image and Energy_image, can be created..

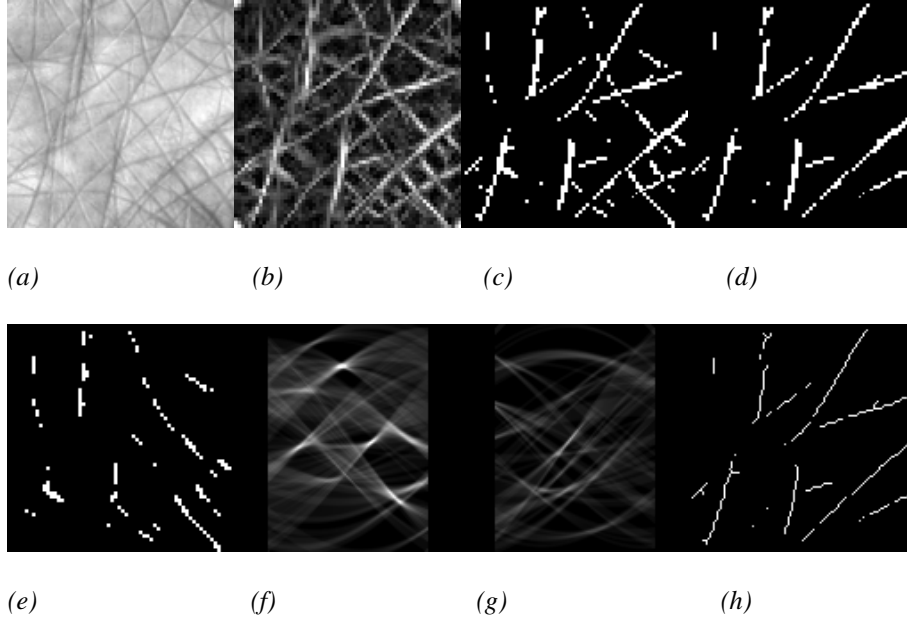


Fig. 1. Images appearing in feature extraction stage: (a) Original image; (b)

Energy_image; (c) *Lines_image*; (d) *LA_image*; (e) *LB_image*; (f) $R(LA_image)$; (g) $R(LB_image)$; (h) Thinning lines of (d).

Fig. 1 shows an example of principal lines extraction extracted by 14×14 MFRAT, which contains some images appearing in this stage. Fig. 1(b) is the *Energy_image* obtained from the original image of Fig. 1(a). It can be seen from Fig. 1(b) that the energies of all palm lines are represented clearly and accurately. In Fig. 1(c), the important lines including principal lines and some strong wrinkles are extracted according to a threshold T . Here, the obtained binary image is called as *Lines_image*, which can be defined as:

$$Lines_image(x, y) = \begin{cases} 0 & \text{if } Energy_image(x, y) < T \\ 1 & \text{if } Energy_image(x, y) \geq T \end{cases} \quad (6)$$

In this step, many wrinkles are removed under the energy criterion. It should be pointed out that T is an important parameter. We sort all pixel values of *Energy_image* in descending order, and select the M^{th} largest pixel value as its adaptive threshold T . In the above example, M was set to 1000.

As we know, *Lines_image* also contains a lot of strong wrinkles. We can further remove them according to the direction criterion. Generally speaking, the directions of most wrinkles markedly differ from that of the principal lines. For instance, if the directions of principal lines belong to $(0^\circ, \dots, \frac{\pi}{2}]$ approximately, the directions of most wrinkles will be at $[\frac{\pi}{2}, \dots, \pi)$ approximately, vice versa. Under this prior knowledge, *Lines_image* is divided into *LA_image* (see Fig. 1(d)) and *LB_image* (see Fig. 1(e)) according to $\theta_{(x,y)}$ of every pixel. It should be noted that those points

whose directions are $\frac{\pi}{2}$ are assigned to both *LA_image* and *LB_image*, i.e.:

$$\begin{aligned} LA_image(x, y) &= 1 & \text{if } line_image(x, y) = 1 & \text{ and } 0^0 < \theta_{(x,y)} \leq \frac{\pi}{2} \\ LB_image(x, y) &= 1 & \text{if } line_image(x, y) = 1 & \text{ and } \frac{\pi}{2} \leq \theta_{(x,y)} < \pi \end{aligned} \quad (7)$$

For *LA_image* and *LB_image*, which one contains principal lines? We applied Radon transform to *LA_image* from 0 to $\frac{\pi}{2}$, and to *LB_image* from $\frac{\pi}{2}$ to π ,

thus two Radon energy maps are created, which are $R[LA_image(x,y)]$ (see Fig. 1(f)) and $R[LB_image(x,y)]$ (see Fig. 1(g)). As we know, the principal lines are generally longer and straighter than the wrinkles, thus the Radon transform energy of principal lines will be greater than the one of the wrinkles. For a binary image $F(x,y)$, there is a criterions that can be adopted to evaluate the Radon transform energy of $R[F(x,y)]$, i.e.:

$$E_{total}(F(x,y)) = \sum_{x=1}^M \sum_{y=1}^N (R[F(x,y)]) \quad (8)$$

Where $E_{total}(F(x,y))$ is the total sum of all values of $R[F(x,y)]$.

By comparing $E_{total}(LA_image(x,y))$ with $E_{total}(LB_image(x,y))$, the above question can be easily answered. The corresponding program code scheme is written as follows:

```

IF  $E_{total}(LA\_image(x,y)) > E_{total}(LB\_image(x,y))$ 
    THEN  $LA\_image$  contains principal lines
    ELSE  $LB\_image$  contains principal lines
END IF

```

In the above example, the principal lines are located in LA_image .

2.2 Extracting LPP feature

Recently, He et al. proposed an appearance-based method called LPP [34]. LPP is a linear approximation of the nonlinear Laplacian Eigenmaps. It seeks to preserve the intrinsic geometry of the data and the local information. In this regards, both PCA and LDA methods are shown to be special cases of LPP method with different similarity matrices. Some experimental results showed that the LPP feature has better performance for recognition than PCA and LDA. Thus, LPP is exploited by our approach. The objective function of LPP is as follows:

$$\min_y \sum_{ij} (y_i - y_j)^2 S_{ij} \quad (9)$$

The objective function with our choice of symmetric weights S_{ij} ($S_{ij} = S_{ji}$) incurs a heavy penalty if neighboring points x_i and x_j are mapped far apart. Therefore, minimizing it is an attempt to ensure that if x_i and x_j are ‘close’ then y_i and y_j are close as well. S_{ij} can be thought of as a similarity measure between objects.

The whole Algorithm of LPP feature extraction can be described as follows:

- (1) The image set (x_i) are projected into the PCA subspace. The transformation matrix of PCA is denoted as W_{PCA} .
- (2) Construct a graph G where the i^{th} node corresponds to the palmprint image x_i . Connect an edge between nodes i and j if x_i and x_j are from the same class. Here, If node i and j are connected, put $S_{ij}=1$, otherwise put $S_{ij}=0$.
- (3) Compute the eigenvectors and eigenvalues for the generalized eigenvector problem:

$$XLX^T w = \lambda DX^T w \quad (10)$$

Where $X=[x_1, x_2, \dots, x_n]$, and D is a diagonal matrix; its entries are column(or row, since S is symmetric) sums of S , $D_{ii} = \sum_j S_{ji}$, $L=D-S$ is the Laplacian matrix. Matrix D provides a natural measure on the data points. The bigger the value D_{ii} (corresponding to y_i) is, the more ‘‘important’’ is y_i .

Let w_0, w_1, \dots, w_{k-1} be the solutions of equation (10), ordered according to their eigenvalues, $0 < \lambda_0 < \lambda_1 < \dots < \lambda_{k-1}$. Thus, the embedding is as follows:

$$y = W^T x \quad (11)$$

Where $W=W_{pca} * W_{LPP}$, y is a k -dimensional vector, W is the transformation matrix.

3. Identification based on restricted fusion

Identification is the one to many matching. In this section, the matching methods and fusion strategy are introduced as follows.

3.1 The matching method of principal lines

Here, we devised a matching algorithm based on pixel-to-area comparison to calculate the similarity of principal lines. Suppose that A is a test image and B is a training image, and the size of A and B is $m \times n$. In A and B , which are all binary images, the value of principal line points is 1. The matching score from A to B is defined as follows:

$$s(A, B) = \left(\sum_{i=1}^m \sum_{j=1}^n A(i, j) \cap \bar{B}(i, j) \right) / N_A \quad (12)$$

where “ \cap ” is the logical “AND” operation, N_A is the number of points on detected principal lines in A , and $\bar{B}(i, j)$ is a small area around $B(i, j)$. In our approach, $\bar{B}(i, j)$ is defined as $B(i+1, j)$, $B(i-1, j)$, $B(i, j)$, $B(i, j+1)$, and $B(i, j-1)$. Obviously, the value of $A(i, j) \cap \bar{B}(i, j)$ will be 1 if $A(i, j)$ and at least one point of $\bar{B}(i, j)$ are principal lines points simultaneously.

In the same way, the matching score from B to A can also be defined as:

$$s(B, A) = \left(\sum_{i=1}^M \sum_{j=1}^N B(i, j) \cap \bar{A}(i, j) \right) / N_B \quad (13)$$

At last, the matching score between A and B is to satisfy:

$$S(A, B) = S(B, A) = \text{Max}(s(A, B), s(B, A)) \quad (14)$$

Theoretically speaking, $S(A, B)$ is between 0 and 1, and the larger the matching score the greater the similarity between A and B . The matching score of a perfect match is 1. Because of imperfect preprocessing, there might have large translations in

practical applications. In order to overcome this problem, we need to vertically and horizontally translate one of feature images and match them again. The ranges of the vertical and horizontal translations are defined from -2 to 2 pixels. The maximum $S(A,B)$ value obtained from translated matchings is considered as the final matching score.

3.2 The distance between LPP features

The distance between two LPP vectors, $Y_i = [y_1^i, y_2^i, \dots, y_d^i]$ and $Y_j = [y_1^j, y_2^j, \dots, y_d^j]$, is defined as follows:

$$d(Y_i, Y_j) = \sum_{k=1}^d \left\| y_k^i - y_k^j \right\|_2 \quad (15)$$

Where $\left\| y_k^i - y_k^j \right\|_2$ denotes the Euclidean distance between the two LPP vectors.

3.3 The restricted fusion strategy

In this subsection, we propose a novel fusion scheme for palmprint identification. Suppose that all training palmprint images come from K classes' palm. And each class contains k_i training palmprint images. Thus the total number of training images is $K * k_i$.

According to the sequence of fusion, two schemes are given. The first fusion scheme is described as follows:

Step 1: For a given test palmprint image A , we extract its principal lines at first. And then, we calculate all matching scores by matching A with all training images, so there will be $K * k_i$ matching scores. We sort all matching scores in descending order, and select the $P1$ images with largest matching scores to construct a sub-database from K classes' training images, so the sub-database contains $P1$ training images. This processing is also depicted in Figure 2.

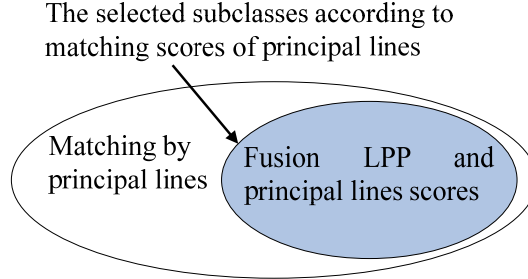


Fig 2. The stage of restricted fusion.

Step 2: Calculating the LPP vectors within all training images. Next, we map A to LPP vector, so we get LPP_A . Next, we calculate the distance between LPP_A and the LPP vectors of selected $P1$ training images. That is to say we get $P1$ matching scores. The distance between LPP_A and the LPP vectors of one training images i denoted as $d(Y_A, Y_i)$. After that, we calculate the normalized distance $dn(Y_A, Y_i)$ by the following formula:

$$dn(Y_A, Y_i) = 1 - \frac{d(Y_A, Y_i)}{\max_{i=1}^P(d(Y_A, Y_i))} \quad (16)$$

Though this normalization, the greater the similarity between A and B , the larger the matching score will be.

Step 3: In this step, fusing the matching scores of principal lines distance and LPP distance by using Product Rule. The last matching score $L(A, B)$ is given as follows:

$$L(A, B) = S(A, B) \times dn(Y_A, Y_B) \quad (17)$$

Step 4: Make classification using Nearest Neighbor classifier.

In the fusion scheme described above, we first calculate the distance of principal lines, and then calculate the similarity of LPP features, so we call this scheme as Principal Lines + LPP (PL+LPP).

The second fusion strategy is similar to previous one. Just the fusion sequence is changed. The Steps are given as follows:

Step 1: Calculating the LPP vectors within all training images. Next, we map A to LPP vector, so we get LPP_A . Next, we calculate the distance between LPP_A and the LPP vectors of all training images. We sort all matching scores in ascending order, and select the $P2$ images with smallest matching scores to construct a sub-database from K classes' training images, so the subclasses contains $P2$ training images.

Normalizing the matching scores by formula (16).

Step 2: we extract principal lines from A . And then, calculate all matching scores by matching A with P2 training images in subclass. Using formula (17) to calculate the last matching score. And exploit the Nearest Neighbor classifier for final classification.

Similarly, we call this fusion scheme as LPP+PL.

Compared with other fusion methods, the proposed method only conducts the fusion in sub-database, rather than the whole database. From another point of view, it can be said that the fusion is restricted.

4. Experimental Results

The proposed method in this paper was tested on the Hong Kong Polytechnic University (PolyU) Palmprint Database. The PolyU Palmprint Database contains 600 grayscale images in BMP image format, corresponding to 100 different palms. In this database, 6 samples from each of these palms were collected in two sessions, where 3 samples were captured in the first session and the second session, respectively. The average interval between the first and the second collection was two months. The resolution of all the original palmprint images is 384×284 pixels at 75 dpi.

Usually, a square region is generally identified as the ROI before feature extraction. Thus the relevant features can be extracted and matched only in this square region. The benefit of this processing is that it can define a coordinate system to align different palmprint images. Otherwise, the matching result would be unreliable without this processing. In this paper, by using the similar preprocessing approach described in literature [1], palmprints were orientated and the ROI, whose size is 128×128 , was cropped.

In this ROI database, three samples of each palm captured in first session were selected to construct a training set (or a template). And three samples of each palm captured in the second session were taken as the test set. Thus, there are total 300 training and test images, respectively.

Table 1 shows the identification results of LPP, LDA, PCA and PCA/w03. It can be seen LPP has the best performance among them.

Table 2 shows the identification results of 2D-LDA and 2D-PCA. Their performances are better than LDA and PCA, respectively.

In our method, there are two parameters that can be adjusted. The first one is the dimension of LPP feature. The second one is the number of training images in constructed sub-database. For the PL+LPP fusion scheme, this number is represented as $P1$. And for the LPP+PL fusion scheme, this number is represented as $P2$.

Table 3 shows the identification results of PL+LPP fusion me scheme. The first row is the dimension of LPP features, and the first column means the number $P1$. From this table, it can be seen that when the dimensions of LPP feature are 90, 100, 110 and 120, and the $P1$ are 7, 8, 9 respectively, the proposed PL+LPP fusion scheme can achieve 100 percent accuracy rate, which is an exciting result.

Table 4 shows the identification results of LPP+PL fusion scheme. From this table, it can be seen that when the dimensions of LPP feature are between 90 and 160, and the $P2$ is set to 9, 100 percent accuracy rate can be obtained.

Figure 3 depicts the performance comparison of proposed schemes and LPP, LDA, PCA/wo3, 2DPCA and 2DLDA, in which the $P1$ is 7 for PL+LPP scheme and $P2$ is 9 for LPP+PL scheme, respectively. Form this figure, it can be seen the proposed fusion methods achieve the best performance.

Table 1. Identification results of LPP, LDA, PCA/wo3 and PCA

	50	60	70	80	90	100	110	120	130	140	150	160
LPP	93.3	94.6	96.7	98	98.7	98.3	98.3	98.3	98.3	98.3	98.3	98.3
LDA	84.6	84	85.7	90	92.7	96.3	96	95.3	94.7	95.3	94.7	94
PCA/wo3	88.3	89	89	90.3	90.7	91.3	91.7	91.7	91.7	91.3	91.7	91.7
PCA	63	66.3	66.3	67	67	68	67.7	67.7	67.7	67.3	67	67.3

Table 2. Identification results of 2DLDA, 2DPCA

	5	6	7	8	9	10	11	12	13	14	15	16
2DPCA	86.7	93.3	95	96.3	96.3	96	96.7	97.3	97.3	97.3	97.3	97
2DLDA	90.7	94.7	96.0	97.3	98	98	98	97.7	97.7	97.7	97.7	97.7

Table 3. Identification results of proposed PL+LPP fusion method

$P1 \backslash$	50	60	70	80	90	100	110	120	130	140	150	160
1	98.7	98.7	98.7	98.7	98.7	98.7	98.7	98.7	98.7	98.7	98.7	98.7
2	98	98	98.7	98.7	98.3	98.3	98.3	98.3	98.3	98.3	98.3	98.3
3	97	98	98.7	99	98.7	98.7	98.7	98.7	98.7	98.7	98.7	98.7
4	97.3	98.3	98	99	99	99	99	99	99	99	99	99

5	97	98	98	99	99.3	99.3	99.3	99.3	99.3	99	99	99
6	96.7	97.7	96.7	98.7	99.7	99.7	99.7	99.7	99.7	99.7	99.3	99.3
7	97	98	98	99	100	100	100	100	100	99.7	99.7	99.7
8	96.7	97.7	98	98.7	100	100	100	100	100	99.7	99.7	99.3
9	96.3	97.3	98	98.7	100	100	100	100	100	99.7	99.7	99.3

Table 4. Identification results of proposed LPP+PL fusion method

P2 \	50	60	70	80	90	100	110	120	130	140	150	160
1	93.3	94.6	96.7	98	98.7	98.3	98.3	98.3	98.3	98.3	98.3	98.3
4	96.7	96.7	97.3	99.7	99.7	99.7	99.7	99.7	99.7	99.7	99.7	99.7
7	97.3	97.7	98.7	99.7	99.7	99.7	99.7	99.7	99.7	99.7	99.7	99.7
9	99.3	99.3	99.7	100								

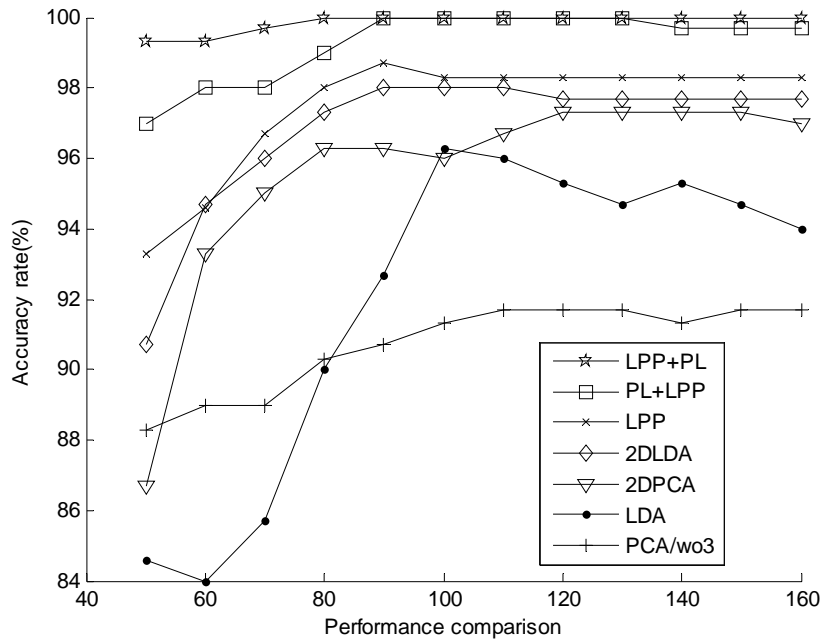


Fig 3. Performance comparison of proposed methods, LPP, LDA, PCA/wo3, 2DPCA and 2DLDA

6. Conclusions

In this paper, we propose two fusion schemes for palmprint identification exploiting principal lines and LPP features. The principal lines can reflect the whole structure of palmprint. And LPP feature can be regarded as the statistic feature of palmprint. Thus, these two features are jointly used to make more reliable identification schemes by exploiting their each advantage. The results of experiments conducted on PolyU palmprint database show that the proposed schemes can achieve 100% accurate recognition rate.

Acknowledgments:

This work was supported by the grants of the National Science Foundation of China, Nos. 60705007 & 60772130, the grant from the National Basic Research Program of China (973 Program), No.2007CB311002, the grants from the National High Technology Research and Development Program of China (863 Program), Nos. 2007AA01Z167 & 2006AA02Z309, the grant of the Guide Project of Innovative Base of Chinese Academy of Sciences (CAS), No.KSCX1-YW-R-30, and the grant of Oversea Outstanding Scholars Fund of CAS, No.2005-1-18

References

- [1] D. Zhang, A. Kong, J. You, M. Wong, Online palmprint identification, *IEEE Trans. Pattern. Anal. Mach. Intell.* 25 (9) (2003) 1041-1050.
- [2] A. Kong, D. Zhang, M. Kamel, Palmprint identification using feature-level fusion, *Pattern Recognition.* 39 (2006) 478-487.
- [3] G.Y. Chen, W.F. Xie, Pattern recognition with SVM and dual-tree complex wavelets. *Image and Vision Computing* 25(6)(2007) 960-966
- [4] Li W, You J Texture-based palmprint retrieval using a layered search scheme for personal identification. *IEEE Transactions on Multimedia* 7(5) (2005) 891-898
- [5] L. Zhang, D. Zhang, Characterization of palmprints by wavelet signatures via directional context modeling, *IEEE Transaction on Systems, Man and Cybernetics, Part B.* 34(3) (2004) 1335-1347.
- [6] C.C. Han, H.L. Cheng, C.L. Lin, K.C. Fan, Personal authentication using palmprint features, *Pattern Recognition* 36(2) (2003) 371-381.

- [7] C. L. Lin, T. C. Chuang, K. C. Fan, Palmprint verification using hierarchical decomposition, *Pattern Recognition*. 38(12) (2005) 2639-2652.
- [8] X.Q. Wu, D. Zhang, K.Q. Wang, B. Huang, Palmprint classification using principal lines, *Pattern Recognition*. 37(10) (2004) 1987-1998.
- [9] X. Q. Wu, D. Zhang, K. Q. Wang, Palm line extraction and matching for personal authentication, *IEEE Transaction on Systems, Man and Cybernetics, Part A*, 36(5) (2006) 978-987.
- [10] L. Liu, D. Zhang, A novel palm-Line detector, *Proceedings of the 5th AVBPA*. (2005) 563-571.
- [11] L. Liu, D. Zhang, J. You, Detecting wide lines using isotropic nonlinear filtering, *IEEE Transaction on Image Procession*. 16(6) (2007) 1584-1595.
- [12] D.S. Huang, W. Jia, D. Zhang, Palmprint verification based on principal lines, *Pattern Recognition* 41(4)(2008) 1215-1428.
- [13] G.M. Lu, D. Zhang, K.Q. Wang, Palmprint recognition using eigenpalms features. *Pattern Recognition Letter* 24(9-10) (2003) 1463-1467.
- [14] X.Q. Wu, D. Zhang, K.Q. Wang Fisherpalms based palmprint recognition. *Pattern Recognition Letter* 24(15)(2003) 2829-2838.
- [15] T. Connie, A.T. B. Jin, M.G.K. On, D. N. C. Ling, An automated palmprint recognition system, *Image and Vision Computing* 23(5) (2005) 501-515.
- [16] D. Hu, G. Feng, Z. Zhou, Two-dimensional locality preserving projecting (2DLPP) with its application to palmprint recognition. *Pattern Recognition* 40(3) (2007) 339-342.
- [17] J. Yang, D. Zhang, J.Y. Yang, B. Niu, Globally Maximizing, Locally Minimizing: Unsupervised Discriminant Projection with Applications to Face and Palm Biometrics. *IEEE Transactions on Pattern Analysis and Machine Intelligence* 29(4) (2007) 650-664.
- [18] A. Kong, D. Zhang, Competitive coding scheme for palmprint verification. *Proc. Of the 17th ICPR vol(1)* (2004) 520-523.
- [19] X.Q. Wu, K.Q. Wang, D. Zhang , Palmprint authentication based on orientation code matching. *LNCS (3546)* (2005) 555-562.
- [20] Z.N. Sun, T.N. Tan, Y.H. Wang, S.Z Li, Ordinal palmprint representation for personal identification, *Proceedings of IEEE International Conference on Computer Vision and Pattern Recognition*. (2005) 279-284.
- [21] W. Jia, D.S. Huang, D. Zhang, Palmprint verification based on robust line orientation code, *Pattern Recognition* 41(5)(2008) 1429-1862
- [22] A. Kumar, D. Zhang, Personal authentication using multiple palmprint representation, *Pattern Recognition*, 38(10) (2005) 1695-1704.

- [23] S. Ribaric, I. Fratric, A Biometric identification system based on eigenpalm and eigenfinger features, *IEEE Trans. Pattern. Anal. Mach. Intell.* 27(11) (2005) 1698-1709.
- [24] A. Kumar, D. Zhang, Personal recognition using hand shape and texture. *IEEE Transactions on Image Processing.* 15(8) (2006) 2454-2461.
- [25] T. Savic, N. Pavesic, Personal recognition based on an image of palmar surface of the hand, *Pattern Recognition*, 40(11)(2007) 3152-3163.
- [26] D.M. Sun, Q. Li, T. Liu, B. He, Z.D. Qiu, A secure multimodal biometric verification scheme, *IWBRS (2005)*, LNCS 3781, 233-240.
- [27] J.G. Wang, W.Y. Yau, A. Suwandy, E. Sung, Person recognition by fusing palmprint and palm vein images based on "Laplacianpalm" representation, *Pattern Recognition* 41(5) (2008) 1531-1544
- [28] X.Y. Jing, Y.F. Yao, D. Zhang, J.Y. Yang, M.Li, Face and palmprint pixel level fusion and kernel DCV-RBF classifier for small sample biometrics recognition, *Pattern Recognition*, 40(11) (2007) 3209-3224.
- [29] D.S.Huang, Wen-Bo Zhao, "Determining the centers of radial basis probabilities neural networks by recursive orthogonal least square algorithms," *Applied Mathematics and Computation*, vol 162, no.1 pp 461-473, 2005.
- [30] D.S.Huang, *Systematic Theory of Neural Networks for Pattern Recognition.* Publishing House of Electronic Industry of China, Beijing, 1996.
- [31] D.S.Huang and S.D.Ma, Linear and nonlinear feedforward neural network classifiers: A comprehensive understanding, *Journal of Intelligent Systems*, Vol.9, No.1, 1-38,1999.
- [32] D.S.Huang, Radial basis probabilistic neural networks: Model and application, *International Journal of Pattern Recognition and Artificial Intelligence*, 13(7), 1083-1101,1999.
- [33] Z. Q. Zhao, D. S. Huang, W. Jia, Palmprint recognition with 2DPCA+PCA based on modular neural networks. *Neurocomputing*, vol 71, pp 448-454
- [34] X.F. He, S.C. Yan, Y.X. Hu, P. Niyogi, H.J. Zhang, Face recognition using laplacianfaces, *IEEE Trans. Pattern Analysis and Machine Intelligence*, 27(3) (2005), 328-340.